# Cardiac MR Findings and Potential Diagnostic Pitfalls in Patients Evaluated for Arrhythmogenic Right Ventricular Cardiomyopathy[1]

*Neda Rastegar, MD*
*Jeremy R. Burt, MD*[2]
*Celia P. Corona-Villalobos, MD*
*Anneline S. te Riele, MD*
*Cynthia A. James, PhD*
*Brittney Murray, MS*
*Hugh Calkins, MD*
*Harikrishna Tandri, MD*
*David A. Bluemke, MD, PhD*
*Stefan L. Zimmerman, MD*
*Ihab R. Kamel, MD, PhD*

Arrhythmogenic right ventricular cardiomyopathy (ARVC) is a familial cardiomyopathy characterized by fibrofatty replacement of the myocardium, ventricular tachycardia, and ventricular dysfunction that affects primarily the right ventricle (RV). This disease is not common but can be seen more frequently in young adults, and clinical manifestations range from no symptoms to lethal arrhythmia and sudden death. The diagnosis of ARVC is challenging and is based on the recently revised international task force criteria. Given the strengths of cardiac magnetic resonance (MR) imaging for depicting the RV, this modality plays an important role in the diagnosis of ARVC. Functional and structural abnormalities of the RV depicted with cardiac MR imaging constitute major and minor criteria in the revised task force criteria. Since the ARVC program was established at our center in 1998, there has been an increased awareness of a number of normal variants that are commonly misinterpreted as showing evidence for ARVC. On the basis of our clinical experience, the overdiagnosis of ARVC appears to reflect two fundamental problems: *(a)* a lack of awareness of diagnostic criteria that identify major and minor variables to be used for the diagnosis of ARVC, and *(b)* a lack of familiarity with the normal variants and mimics that may be misinterpreted as showing evidence of ARVC. The purpose of this article is to review the typical patterns of ventricular involvement in ARVC at cardiac MR imaging and to compare those with the patterns of normal variants and other diseases that can mimic ARVC. *Online supplemental material is available for this article.*



**Abbreviations:** ARVC = arrhythmogenic right ventricular cardiomyopathy, LV = left ventricle, RV = right ventricle, RVOT = right ventricular outflow tract, SSFP = steady-state free precession

**RadioGraphics 2014;** 34:1553–1570

**Published online** 10.1148/rg.346140194

**Content Codes:** CA MR

[1]From the Russell H. Morgan Department of Radiology and Radiological Sciences (N.R., J.R.B., C.P.C., S.L.Z., I.R.K.) and Division of Cardiology (C.A.J., B.M., H.C., H.T.), Johns Hopkins University School of Medicine, 600 N Wolfe St, MRI 143, Baltimore, MD 21287; Division of Cardiology, University Medical Center Utrecht, Utrecht, the Netherlands (A.S.t.R.); and Department of Radiology and Imaging Sciences, National Institutes of Health Clinical Center, Bethesda, Md (D.A.B.). Recipient of a Cum Laude award for an education exhibit at the 2011 RSNA Annual Meeting. Received February 13, 2013; revision requested April 11 and received April 21, 2014; accepted April 21. For this journal-based SA-CME activity, the author H.C. has provided disclosures (see p 1568); all other authors, the editor, and the reviewers have disclosed no relevant relationships. J.R.B. supported by the Radiological Society of North America (grant RF1106). H.C. supported by St. Jude Medical Foundation. **Address correspondence to** I.R.K. (e-mail: *ikamel@jhmi.edu*).

[2]**Current address:** Radiology Specialists of Florida, Florida Hospital, Orlando, Fla.

Scan this code for access to supplemental material on our website.

**TEACHING POINTS**

*See last page*

## SA-CME LEARNING OBJECTIVES

*After completing this journal-based SA-CME activity, participants will be able to:*

- Identify the task force criteria for ARVC.
- List potential mimics of ARVC and the pitfalls in its identification, in the order of their frequency.
- Discuss how to differentiate ARVC from its mimics.

*See www.rsna.org/education/search/RG.*

## Introduction

Arrhythmogenic right ventricular cardiomyopathy (ARVC) is an inherited disease characterized by fibrofatty replacement of the myocardium, life-threatening ventricular arrhythmias, and cardiac dysfunction, predominantly of the right ventricle (RV). Inheritance of one or more desmosomal mutations leads to the disease, and the inheritance follows

**Table 1: Original and Revised Imaging Task Force Criteria for the Diagnosis of ARVC**

| 1994 Task Force Criteria* | 2010 Task Force Criteria |
|---|---|
| Major criteria | |
| Severe RV dilatation and reduction of RV ejection fraction with or without (or with only mild) LV impairment<br>Localized RV aneurysms (akinetic or dyskinetic areas with diastolic bulging)<br>Severe segmental dilatation of the RV | Two-dimensional echocardiographic criteria<br>Regional RV akinesia, dyskinesia, or aneurysm<br>Plus one of the following (end-diastolic): *(a)* PLAX RVOT ≥ 32 mm or PSAX RVOT ≥ 36 mm, or *(b)* fractional area change ≤ 33%†<br>MR imaging criteria<br>Regional RV akinesia, dyskinesia, or dyssynchrony‡<br>Plus one of the following: *(a)* ratio of RV end-diastolic volume to body surface area ≥ 110 mL/m$^2$ (male) or ≥ 100 mL/m$^2$ (female), or *(b)* RV ejection fraction ≤ 40%<br>RV angiographic criteria<br>Regional RV akinesia, dyskinesia, or aneurysm |
| Minor criteria | |
| Mild global RV dilatation and/or ejection fraction reduction with normal LV<br>Mild segmental dilatation of the RV<br>Regional RV hypokinesia | Two-dimensional echocardiographic criteria<br>Regional RV akinesia, dyskinesia, or aneurysm<br>Plus one of the following (end-diastolic): *(a)* PLAX RVOT ≥ 29 to < 32 mm or PSAX RVOT ≥ 32 to < 36 mm, or *(b)* fractional area change of 33%–40%†<br>MR imaging criteria<br>Regional RV akinesia, dyskinesia, or dyssynchrony‡<br>Plus one of the following: *(a)* ratio of RV end-diastolic volume to body surface area ≥ 100 to < 110 mL/m$^2$ (male) or ≥ 90 to < 100 mL/m$^2$ (female), or *(b)* RV ejection fraction > 40% to ≤ 45%<br>RV angiographic criteria<br>Regional RV akinesia, dyskinesia, or aneurysm |

Sources.—References 5 and 11.

Note.—LV = left ventricle, PLAX = parasternal long axis, PSAX = parasternal short axis, RVOT = RV outflow tract.

*Global or regional dysfunction and structural alterations.

†RVOT values corrected for body size.

‡Dyssynchronous RV contraction.

an autosomal dominant pattern with variable penetrance. The prevalence of ARVC ranges from 0.05% to 0.1%; and in North America, ARVC is equally common in male and female subjects (1,2). In spite of the low prevalence, evaluation for ARVC accounts for a disproportionately high percentage of referrals to cardiac magnetic resonance (MR) imaging centers (3). This observation is likely due to the fact that ARVC may first manifest with fatal arrhythmias in a relatively young individual (4,5). Patients typically present between the 2nd and 4th decades of life. However, cases of ARVC have been reported with patient ages ranging from 8 to 80 years (mean age, 33 years) (6). ARVC is one of the most common causes of sudden death in those aged 35 years and younger, especially in athletes; and ARVC causes as many as 10% of the deaths from undiagnosed cardiac disease in subjects younger than 65 years old (7,8). Unfortunately, in 20%–50% of cases, sudden cardiac death is the first manifestation of ARVC (2,9).

The purpose of this article is to review the typical patterns of ventricular involvement in ARVC at cardiac MR imaging and compare those with the patterns of normal variants and other diseases that can mimic ARVC, to help radiologists and other imagers avoid misdiagnosis. First, the diagnostic criteria for ARVC are reviewed. Then our imaging protocol, the task force criteria for ARVC, and other ARVC findings are detailed. Various normal variants that can be mischaracterized as findings of ARVC are covered. Finally, the pathologic conditions that mimic findings of ARVC are discussed.

## Diagnostic Criteria for ARVC

Diagnostic criteria for ARVC were initially described by the international task force of cardiomyopathies in 1994; these criteria are known as the task force criteria (5,10,11). Structural and functional ventricular abnormalities at echocardiography or cardiac MR imaging, electrocardiographic abnormalities, a personal history of

**Table 2: Cardiac MR Imaging Protocol**

| Parameter | Imaging Sequence | | |
|---|---|---|---|
| | "T1" Dark Blood | Bright-Blood Cine | Delayed Enhancement |
| Mode | Two-dimensional | Two-dimensional | Two-dimensional |
| Plane of imaging | Axial, short axis | Short axis, horizontal long axis, RVOT, axial | Short axis, axial |
| Type | Fast spin-echo with or without fat suppression | SSFP | Segmented gradient echo |
| TR (msec)/TE (msec) | 1–2 RR/28 | 2.6/1.3 | 7.2/3.2 |
| Flip angle (degrees) | 180 | 40–80 | 25 |
| Section thickness (mm) | 5 | 8 | 8–10 |
| Section gap (mm) | … | 2 | 2 |
| Field of view (cm) | 24–36 | 30–40 | 30–36 |
| Matrix (frequency phase) | 144–256 × 192–256 | 192–256 × 160–192 | 130–256 × 176–192 |
| Inversion time (msec) | … | … | 150–250 |
| Temporal resolution (msec) | … | 30–40 | … |

Note.—RR = R wave–to–R wave interval, SSFP = steady-state free precession, TE = echo time, TR = repetition time.

arrhythmia, a family history of sudden death or known ARVC, and histopathologic changes at biopsy were the categories of findings that made up the original task force criteria (5). These criteria had the advantage of high specificity (high true-negative rate for subjects without ARVC) but were limited by low sensitivity (low true-positive rate for subjects with ARVC), especially in the diagnosis of familial and early disease (5,9). The major or minor imaging criteria of the original 1994 task force criteria included the presence of global or regional RV dilatation (evaluated subjectively), RV microaneurysm, or regional hypokinesia (3).

In 2010, these task force criteria were revised, with the objective of improving the sensitivity and specificity, and therefore the accuracy, for the diagnosis of ARVC (3,12). The revised criteria included quantitative and qualitative parameters for cardiac MR imaging, Holter monitoring, electrocardiography, and signal-averaged electrocardiography, as well as genetic test results. Microaneurysms of the RV (dyskinesia in systole with persistent diastolic bulging) and segmental RV dilatation were removed from the imaging criteria because these two criteria were subjective and difficult to interpret (3–5,10,11) (Table 1). In this revised version of the task force criteria, the combination of *(a)* regional RV wall motion abnormality, such as akinesia, dyskinesia, or dyssynchrony, and *(b)* reduced global RV function or increased RV end-diastolic volume index (quantitative assessment) is necessary to meet major or minor criteria at cardiac MR imaging (4,5). The addition of genetic test results to the task force criteria increases the sensitivity for diagnosis in subjects with familial disease (5,9).

Despite the strengths of cardiac MR imaging in the diagnosis of ARVC, a high potential for misdiagnosis remains because of the inherent difficulties in quantitative and qualitative assessment of the RV (13). Although cardiac MR imaging is considered the standard of reference for determining the structure and function of the RV and the LV, the use of cardiac MR imaging alone is not the standard of reference for the diagnosis of ARVC. Instead, the task force criteria emphasize the use of multiple diagnostic tests (4,5). Additionally, normal variants as well as other disorders of the RV mimic the findings of ARVC at cardiac MR imaging. Incorrect interpretation of cardiac MR imaging findings can have serious consequences for the patient, resulting in patient anxiety, inappropriate invasive therapy, including implantable cardiac defibrillator placement, and, not infrequently, unnecessary workup and treatment of the patient's relatives. For this reason, physicians, especially radiologists and cardiologists, should become familiar with how to diagnose this disease and should be aware of the pathologic and physiologic conditions that have similar manifestations.

## Cardiac MR Imaging: Protocol, Diagnostic Criteria, and Other Findings

### MR Imaging Protocol

The cardiac MR imaging studies were performed on a 1.5-T imager (Avanto; Siemens, Erlangen, Germany). Our cardiac MR imaging protocol for ARVC evaluation is shown in Table 2.

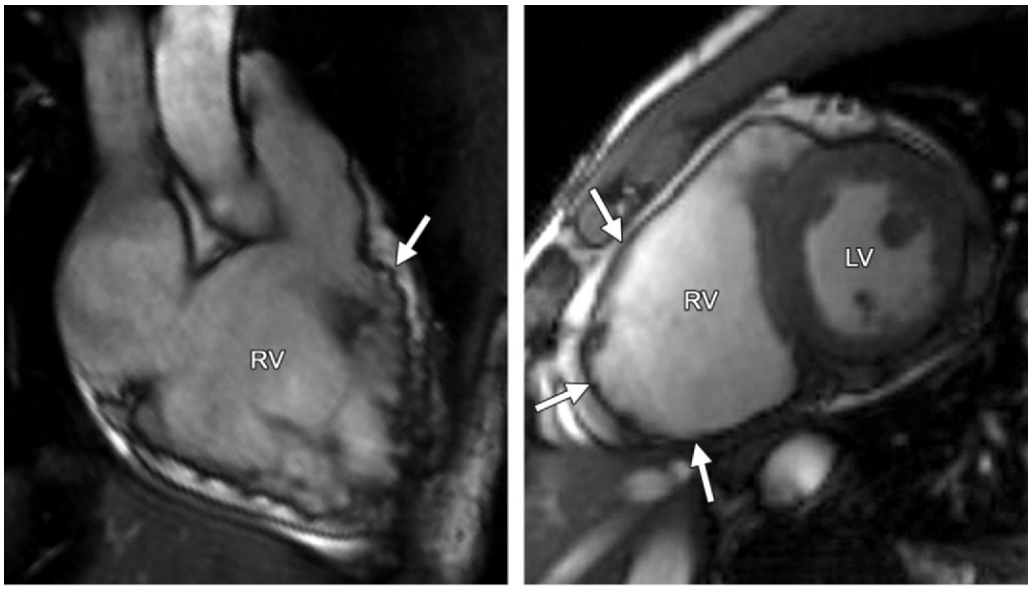


a. b.

**Figure 1.** Common locations of RV wall motion abnormalities in ARVC: cardiac MR images of a 23-year-old man with ARVC. **(a)** Bright-blood SSFP MR image obtained in the RVOT plane shows a microaneurysm in the RV free wall (arrow). **(b)** Short-axis bright-blood SSFP MR image shows the common locations (arrows) of RV wall motion abnormalities in patients with ARVC.

## Task Force Criteria for ARVC

To meet diagnostic cardiac MR imaging criteria according to the revised task force criteria, any RV wall motion abnormality must be accompanied by quantitative RV dilatation or reduced function. Regional wall motion abnormalities are defined as akinesia (complete loss of movement), dyskinesia (movement of a myocardial segment outward in systole), or dyssynchrony (movement of a myocardial segment outward in systole and inward in diastole). Sex-specific cutoffs for normalized RV volumes and RV ejection fraction are used (Table 1). The severity of RV dilatation (quantitatively) or RV dysfunction determines whether cardiac MR imaging findings meet major or minor criteria. The most common task force criteria finding in patients with ARVC is a regional RV wall motion abnormality, which is frequently seen in the basal and mid free wall, the inferior wall, including the acute angle of the RV, and the RVOT (12,14) (Movies 1, 2 [online]) (Fig 1). In our experience, axial cine images are best for evaluation of the RV free wall, short-axis cine images for the inferior wall and angle of the RV, and RVOT views for the inferior wall. Regional wall motion abnormalities should be confirmed on images obtained in more than one imaging plane.

## Other Non–Task Force Criteria Findings of ARVC

In addition to the task force criteria findings, several other findings may be encountered in patients with ARVC. Some of these findings are categories of wall motion abnormalities that are not part of the task force criteria. Microaneurysms of the RV, a severe form of wall motion abnormality, are small focal bulges in the wall of the RV that persist in systole and diastole (Fig 1) (15). Another type of focal wall motion abnormality is the "accordion sign," which is a focal crinkling of the RVOT or the subtricuspid region of the RV free wall that becomes more prominent during systole (16). In prior studies, investigators showed that the presence of the accordion sign helps in diagnosing ARVC in family members who eventually meet diagnostic criteria. In addition, there is an association between this sign and the severity of the disease (16).

Another finding in subjects with ARVC is infiltration of fat. On the basis of the pathogenesis and the nature of myocardial tissue replacement, two morphologic features can be seen: *(a)* fatty tissue (fatty or lipomatous pattern), and *(b)* fibrous and fatty tissue (fibrofatty or fibrolipomatous pattern) (17–19). The fatty pattern is associated with preserved myocardial thickness, whereas in the fibrofatty pattern, there is marked thinning of the myocardium (7,17,20,21) (Fig 2). Intramyocardial fat is more commonly seen in the basal and mid free wall, the RVOT, and the lateral apex and occasionally is seen in the inferoseptal portion of the RV, the RV trabeculae, and the moderator band (12,15,22,23). Fibrosis is usually seen in the same place as fat and may result in delayed enhancement after contrast material administration. A strong association exists between

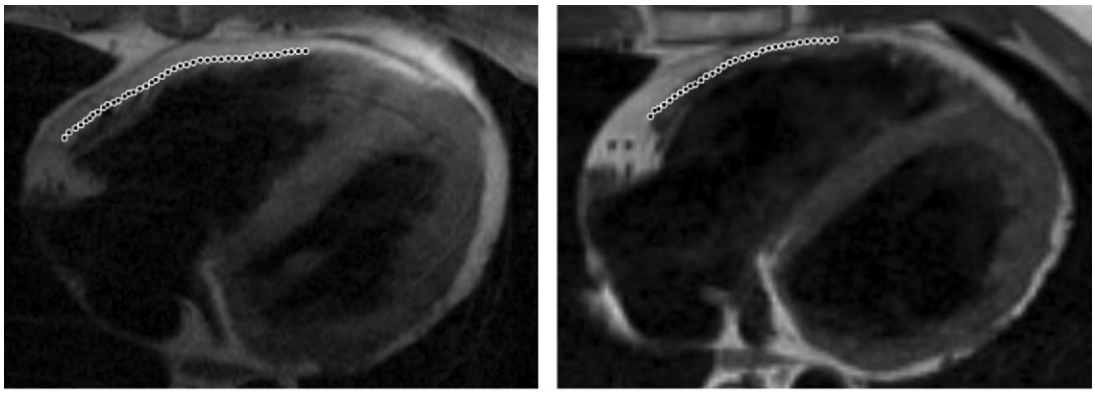

a. b.

**Figure 2.** Infiltration of fat in the RV of two patients with a history of ARVC. Axial T1-weighted fast spin-echo non–fat-suppressed MR images of a 52-year-old man **(a)** and a 37-year-old man **(b)** show fingerlike projections of fat, which has high signal intensity, in the RV wall. Note that the pattern of infiltration of fat resulted in myocardial thinning in **a**, but myocardial thickness is preserved in **b**. The dotted line indicates the expected location of the myocardial wall.

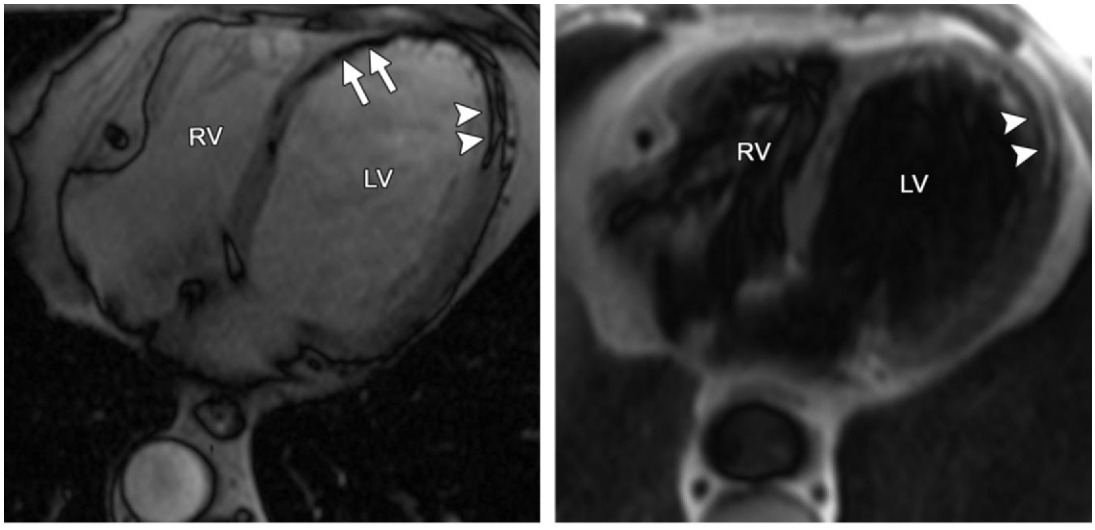


a. b.

**Figure 3.** Fat deposition from a healed myocardial infarction in a 65-year-old man with a history of myocardial infarction. Axial bright-blood SSFP **(a)** and T1-weighted fast spin-echo non–fat-suppressed **(b)** MR images show increased signal intensity in the subendocardial region of the LV apex (arrowheads) secondary to fat deposition in the setting of a chronic myocardial infarction. Etching artifact (arrows in **a**), a cardiac MR imaging finding that results from the loss of signal in voxels that contain both fat and water protons, surrounds the apical fat on bright-blood MR images.

the extent of delayed enhancement and RV dysfunction (23). However, to date, the pattern of fatty deposition and fibrosis and also the effect of the amount of epicardial fat on the diagnosis of ARVC are unknown.

## Normal Variants Mischaracterized as Findings of ARVC

### Myocardial Fat

Although myocardial fat and wall thinning can be found in patients with ARVC at cardiac MR imaging (14,22,24,25), these findings are not diagnostic for ARVC. The presence of myocardial fatty or fibrofatty infiltration is not included in either the revised or the original task force criteria because of *(a)* artifactual fat resulting from limited imaging techniques (22) and *(b)* the presence of fatty infiltration in physiologic (20–24) and other pathologic states, such as healed myocardial infarction (18,24–30) (Fig 3), cardiac lipoma (31,32), lipomatous hypertrophy of the interatrial septum (33), tuberous sclerosis complex (34), and dilated cardiomyopathy. Isolated and marked lipomatous infiltration of the RV appears to be a separate condition from ARVC

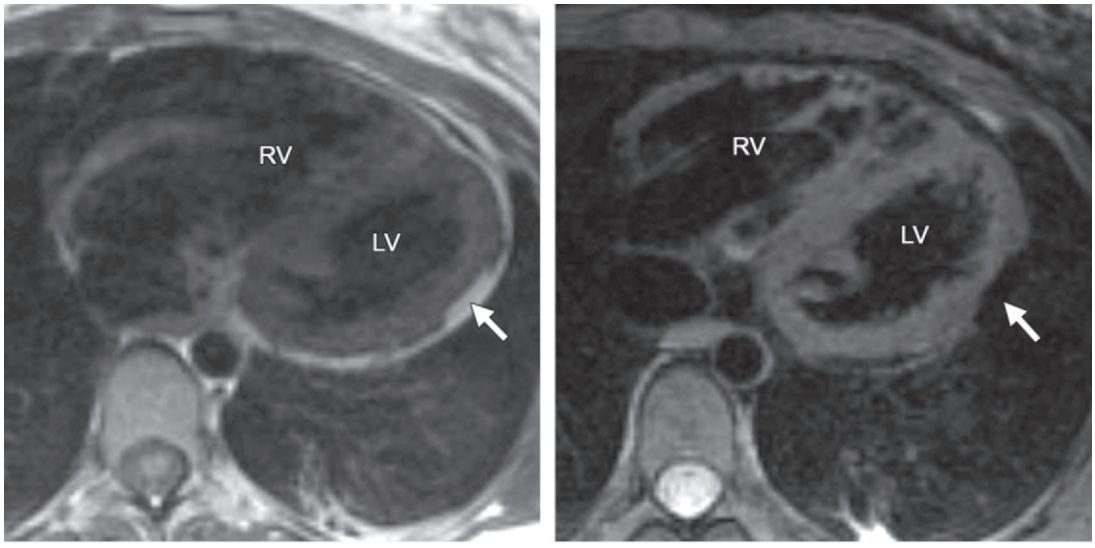


**Figure 4.** Infiltration of fat in the LV of a 30-year-old man with a history of biventricular ARVC. Axial T1-weighted fast spin-echo non–fat suppressed **(a)** and T2-weighted fat-saturated **(b)** MR images show the typical infiltration of fat (arrow) in the lateral wall of the LV.

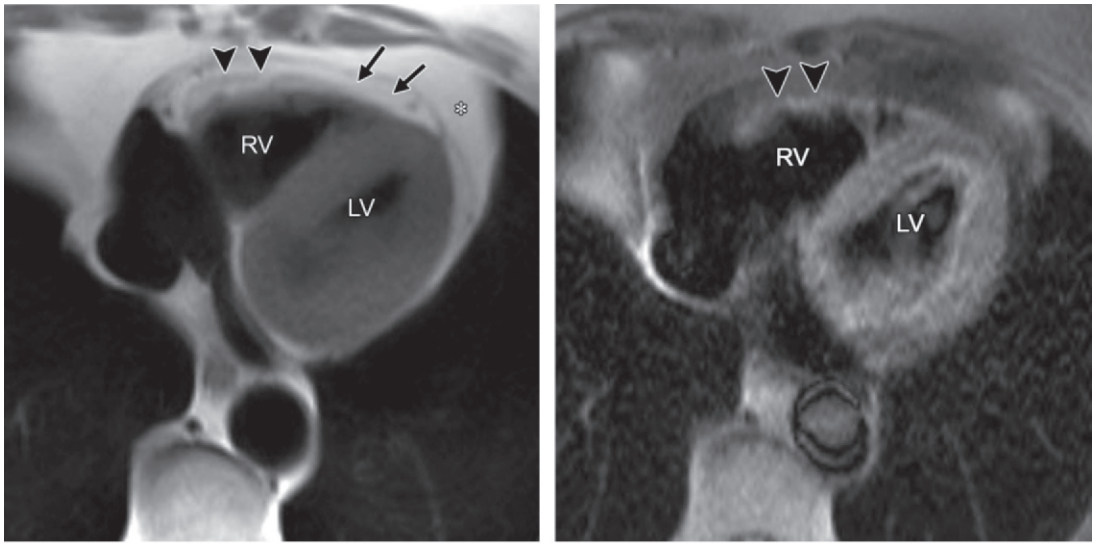


**Figure 5.** Incidental finding of RV fat in a 66-year-old woman with no history of ARVC. Axial T1-weighted fast spin-echo non–fat-saturated **(a)** and T2-weighted fat-saturated **(b)** MR images show prominent mediastinal fat (* in **a**), pericardial fat (arrows), and epicardial fat (arrowheads). Note that the epicardial fat extends into the RV free wall. Fat can be seen as areas of high signal intensity on T1-weighted images **(a)** and as areas of low signal intensity on fat-saturated images **(b)**. Note that the subendocardium is spared, and the RV size is normal.

(35). Given that fibrofatty change is the histopathologic hallmark of ARVC, many imagers are inclined to look for it to help support the diagnosis. However, the presence of RV myocardial fat at cardiac MR imaging should not be interpreted independently. We recommend the evaluation of fibrofatty infiltration only as a secondary assessment after the evaluation of the more reliable functional and structural assessment of the RV as defined by the task force criteria (13,36).

Teaching Point

***Infiltration of Fat in ARVC.***—In ARVC, fat can be deposited in both the RV (Fig 2) and the LV (Fig 4) (12). High-resolution two-dimensional fast spin-echo T1-weighted black-blood MR images with and without fat saturation can be used to identify fatty infiltration of the myocardium. Fat is recognized as a high-signal-intensity structure within the adjacent low-signal-intensity myocardium, with a characteristic loss of signal with the use of fat-saturated pulse sequences (30). How-

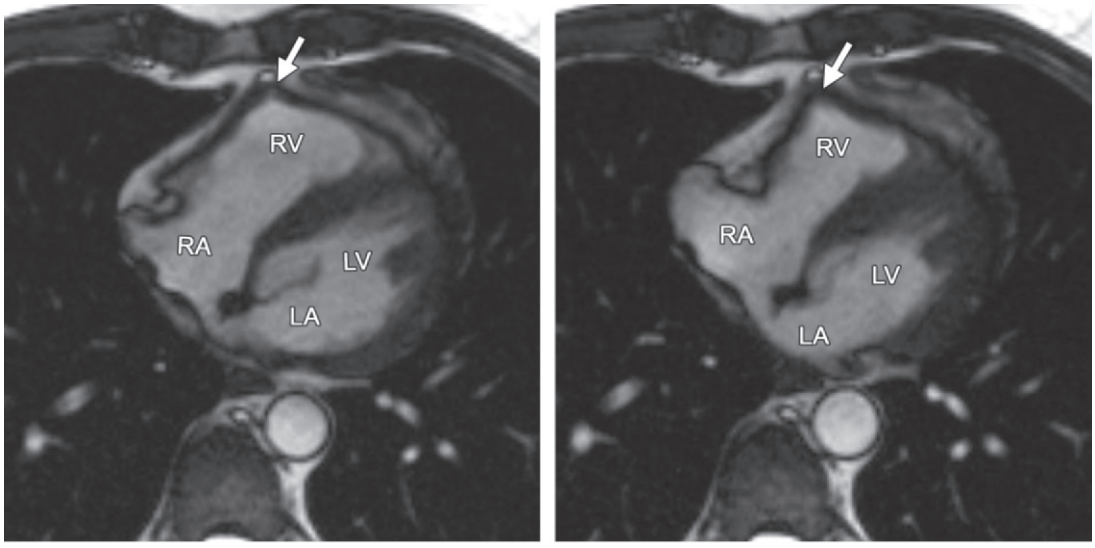


a. b.

**Figure 6.** RV free wall tether in a 50-year-old man with no history of ARVC. Axial end-diastolic **(a)** and end-systolic **(b)** bright-blood SSFP MR images show tethering (arrow) of the pericardium along the RV free wall to the posterior sternum, which may be misinterpreted as dyskinetic RV wall motion. *LA* = left atrium, *RA* = right atrium.

ever, blurring of the fat-myocardial interfaces with the use of fast spin-echo sequences is a limitation of this approach, and relatively large amounts of fat are required for recognition at cardiac MR imaging (30). Fat deposition on cardiac MR images tends to have an infiltrative pattern with fingerlike projections disrupting the normal smooth contour of the RV (Fig 2). In ARVC, the most common locations of infiltration of fat are the epicardial RV and LV free walls and, occasionally, the inferoseptal portion of the RV, the RV trabeculae, and the moderator band (22,23).

***Non-ARVC Fatty Infiltration of the RV.***—Tansey et al (37) reported that the incidence of physiologic myocardial fat deposition at autopsy of subjects who died of noncardiac causes was as high as 85%. Physiologic fat usually spares the subendocardium and characteristically increases the total thickness of the involved myocardium (Fig 5).This is in contrast to ARVC, in which fat replaces normal myocardium, resulting in an unchanged or thinner wall thickness (22). Physiologic fat is seen more commonly in the RV than in the LV, and the incidence of physiologic fat is higher in obese, older, and female individuals (22,37). In the RV, the most common locations of physiologic fat are in the free wall and the RVOT, resulting in considerable overlap with the locations of fat in ARVC (18,22). An important limitation of the current literature is the lack of correlation between autopsy findings and cardiac MR imaging findings. To date, the sensitivity and accuracy of cardiac MR imaging in the depiction of the physiologic fat commonly seen at autopsy are unknown. Subjects with non–ARVC-related fat (without underlying cardiac disease) have normal RV size and function, findings that can help distinguish such subjects from those with ARVC (35).

Teaching Point

## RV Free Wall Tether

The appearance of a band of pericardial connective tissue that joins the anterior free wall of the RV to the posterior aspect of the sternum may be seen in some normal subjects, a finding that results in a tethered appearance of the RV (Fig 6). At cine imaging, the tethered portion of the RV free wall remains static in location, whereas the adjacent RV myocardium contracts normally (Movie 3 [online]). In our experience, this finding may be misinterpreted as dyskinetic motion of the RV free wall related to ARVC. Because this abnormality is not related to intrinsic myocardial dysfunction but rather is an anatomic variant, it should not be misinterpreted as an RV wall motion abnormality. These patients have a triangular-shaped RV free wall, with the apex of the triangle directed toward the posterior portion of the sternum. Not infrequently, a localized area of pericardial thickening can be identified. This triangular region persists on systolic images.

Teaching Point

## Pectus Excavatum

In pectus excavatum, the distance between the sternum and the thoracic spine is decreased, thereby shifting the mediastinum to the left and causing a distorted appearance of the otherwise

normal RV, which can potentially be mistaken for ARVC. Because patients being evaluated for ARVC are frequently young and otherwise healthy, some will have undiagnosed pectus excavatum at the time of cardiac MR imaging. Pectus excavatum deformity of the chest wall, which is reported to account for 90% of cases of congenital chest wall deformity, results in restricted motion of the basolateral and inferolateral walls of the RV (38). Pectus excavatum also causes narrowing of the RV base and relative enlargement of the RV apex and the RVOT, potentially leading to a misdiagnosis of ARVC (Movie 4 [online]). The RV takes an elongated shape, which we refer to as the "banana-shaped RV" (Fig 7). In addition, distortion of the RV base on the short-axis images may result in incorrect quantitative functional analysis. Careful evaluation of the RV base is recommended in patients with pectus excavatum, and apparent hypokinesia at this location should be discounted if motion is obviously restricted by the sternum (Fig 8). Quantitative analysis of the short-axis images must be performed by using reference sections from the horizontal long-axis and RV inflow-outflow planes to ensure that sections from the right atrium are not included in the RV volume.

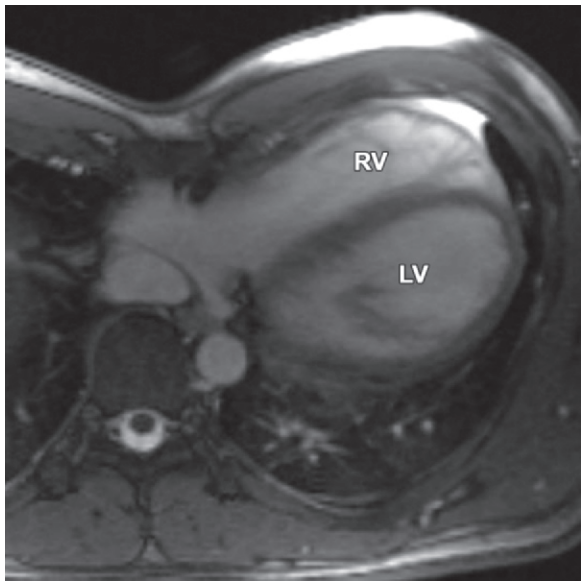


**Figure 7.** Banana-shaped RV in a 40-year-old man with pectus excavatum. Axial bright-blood SSFP MR image obtained to rule out ARVC shows a banana-shaped appearance of the RV. No findings were suggestive of ARVC.

## Apicolateral Bulge

Subjective assessment of RV wall motion is challenging because of the variability of the RV shape. Regional RV wall motion abnormality is a necessary component for the diagnosis of ARVC in the revised task force criteria. Frequent sites for regional RV wall motion abnormality in ARVC include the basal and mid segments of the free wall, the inferior wall, including the acute angle of the RV, and the RVOT (12) (Fig 1) (Movies 1, 2 [online]). However, the findings from studies performed by Sievers et al (39) and Fritz et al (40) showed a high prevalence of subjective regional RV wall motion abnormality at cardiac MR imaging in healthy volunteers. The most frequent site of apparent abnormality, which was seen in 79% of the healthy volunteers, was at the insertion site of the moderator band in the apicolateral wall (Fig 9) (Movie 5 [online]). We describe this finding as the "apicolateral bulge." In our experience, wall motion abnormality in the apicolateral wall of the RV does not occur as an isolated finding of ARVC. However, because of the high incidence of apicolateral bulge, it may be seen in some ARVC patients who would also have additional areas of regional wall motion abnormalities. The presence of an apicolateral bulge in isolation should therefore be considered a normal variant and, in the absence of other regional RV wall motion abnormalities, should not be used to meet major or minor revised task force criteria.

## Apical Aneurysm

Normally, the cardiac apex is formed by the LV alone. A common anatomic variation is for both the RV and LV to form separate apices, a variant that has been called a "butterfly apex" (29). Sometimes, unusual prominence of the RV apex can be inadvertently called dyskinetic or aneurysmal. In our experience, the RV apex and apicolateral segments are not typically involved in isolation in ARVC, an observation that helps to avoid misdiagnosis in this situation. In addition, the butterfly apex can be distinguished from a

**Figure 8.** Pectus excavatum compared with ARVC: **(a–c)** MR images of a 40-year-old man with pectus excavatum, and **(d–f)** MR images of a 54-year-old man with a history of ARVC. The axial end-diastolic **(a, d)** and short-axis bright-blood SSFP **(b, c, e, f)** MR images show that both patients have an elongated appearance of the RV, which may result in a false-positive diagnosis of ARVC in patients with pectus excavatum. Prominence of the RVOT (black arrow in **a,** white arrow in **b**) and the RV apex (arrowhead in **c**) can be seen because of the extrinsic compression of the base of the RV by the pectus abnormality (white arrow in **a**). These features can be distinguished from those in ARVC **(d–f)**, in which there is dilatation of the entire RV, involving the base through the apex.

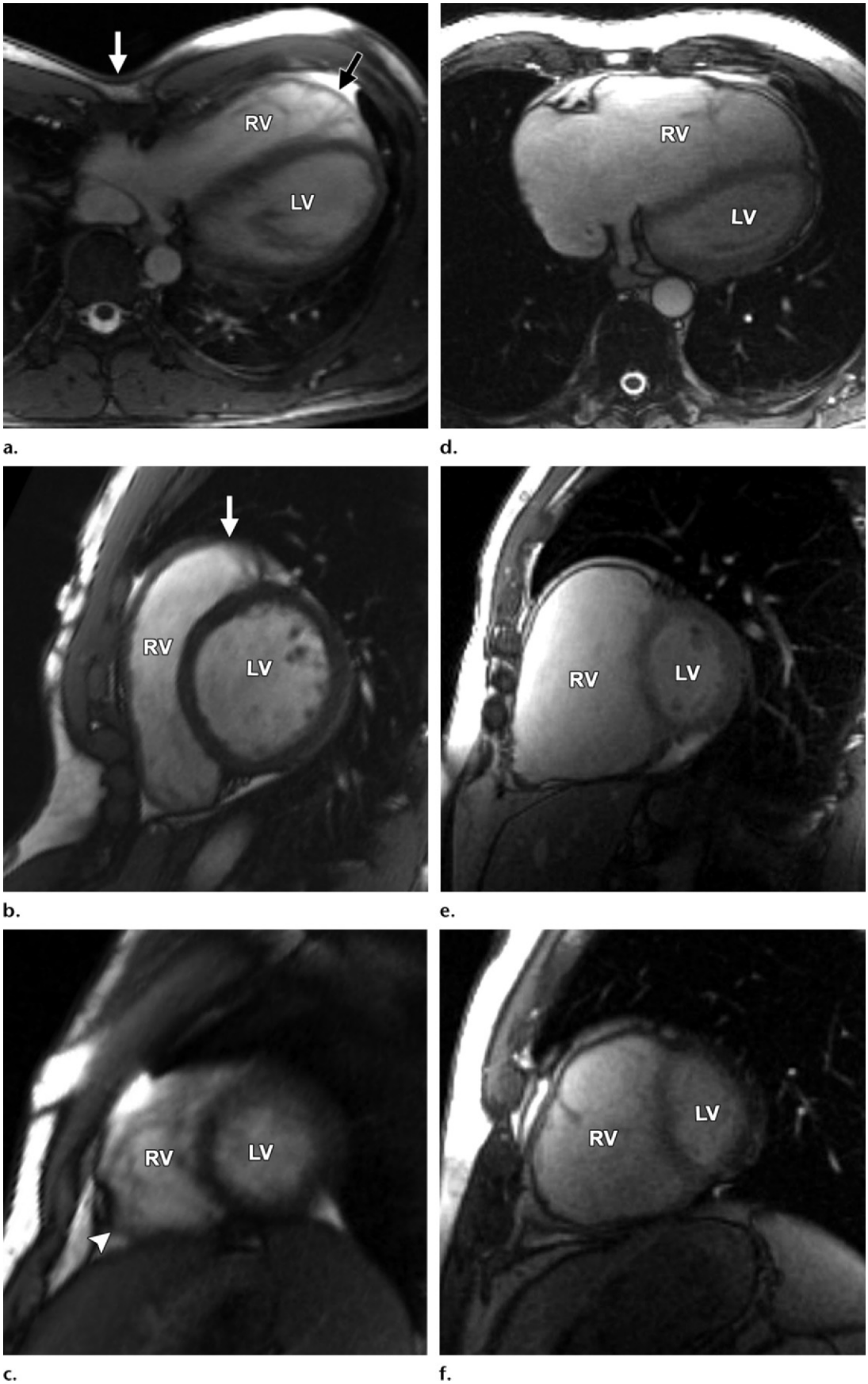
RV
LV
a.
RV
LV
d.
RV
LV
b.
RV
LV
e.
RV
LV
c.
RV
LV
f.

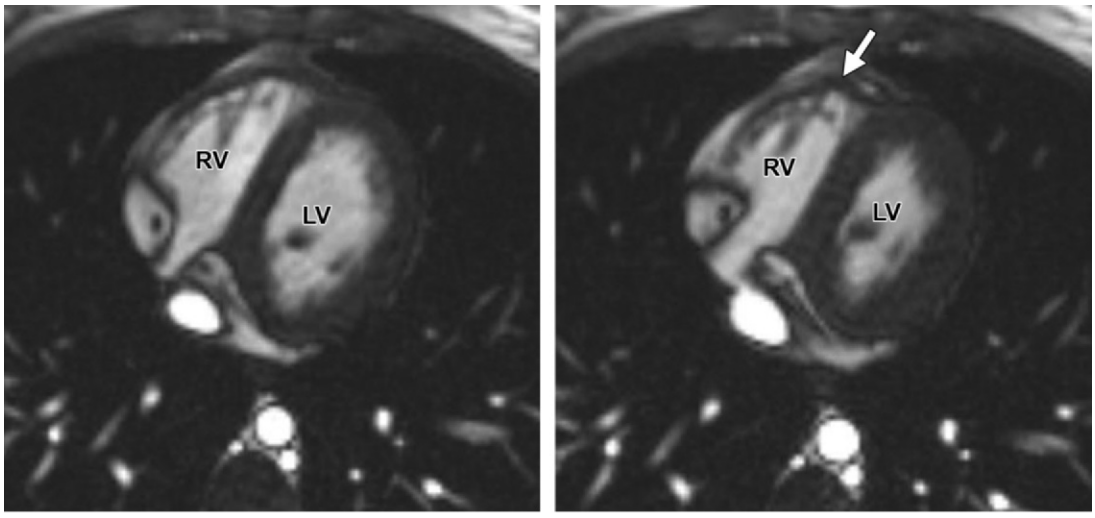


**Figure 9.** Apicolateral bulge in a 17-year-old female adolescent with no history of ARVC. Axial end-diastolic **(a)** and end-systolic **(b)** bright-blood SSFP MR images were obtained because of the patient's episodes of syncope. An apicolateral bulge (arrow in **b**) is depicted adjacent to the insertion of the moderator band on the RV free wall, a finding that can be seen in normal subjects.

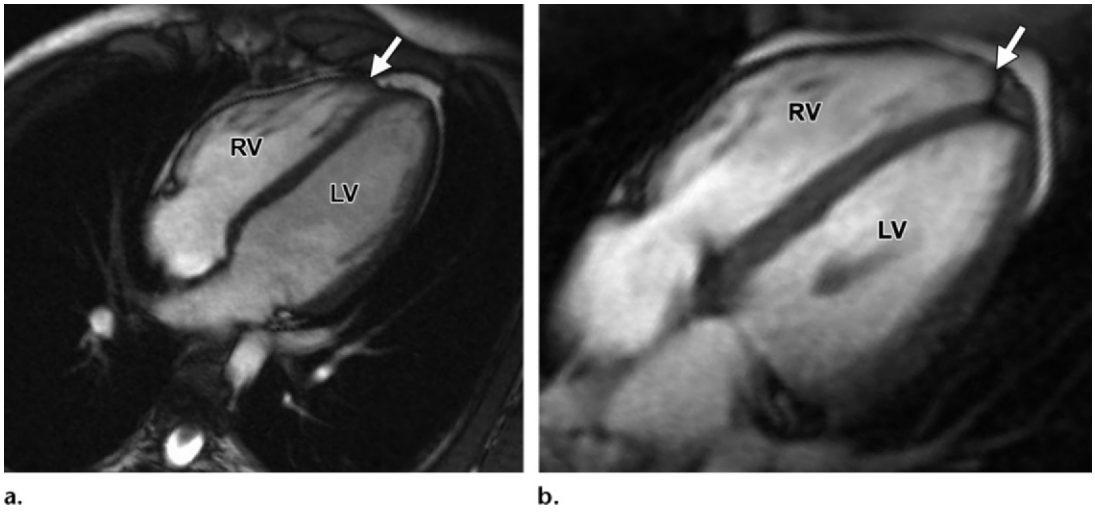


**Figure 10.** Butterfly apex compared with normal cardiac apex. **(a)** Horizontal long-axis bright-blood SSFP MR image of a 41-year-old man with no history of ARVC shows a normal cardiac apex (arrow) that is formed by the LV only. **(b)** Horizontal long-axis bright-blood MR image of a 15-year-old female adolescent who received a misdiagnosis of ARVC because of what was thought to be an RV apical aneurysm (arrow). However, this structure is a normal-variant butterfly apex, and the patient had no evidence of ARVC.

dyskinetic or aneurysmal segment because it will have normal wall motion during systole with the same systolic thickening and diastolic thinning as seen in adjacent normal RV segments (Fig 10).

## Pulmonary Valve Sinuses

Abnormalities of the RVOT are common in patients with ARVC (41,42). Dilatation and dyskinesia of the RVOT are frequently seen (Fig 11). When imaged in the short-axis or RV inflow-outflow planes, the pulmonary valve sinuses can give the appearance of dyskinetic systolic wall motion in the region of the RVOT. These sinuses fill with blood during systole, which results in a normal systolic bulge. Pulmonary valve leaflets are frequently not well seen on cine SSFP (bright-blood) images, which makes interpretation of the findings in this region challenging. Misinterpretation is best avoided by closely evaluating the exact site of dyskinesia with the RV inflow-outflow plane of imaging. If the bulging segment is located above the annulus of the pulmonary valve, superior to the RVOT, then it represents normal outpouching of the pulmonary valve sinuses, whereas wall motion abnormalities in ARVC occur below this level

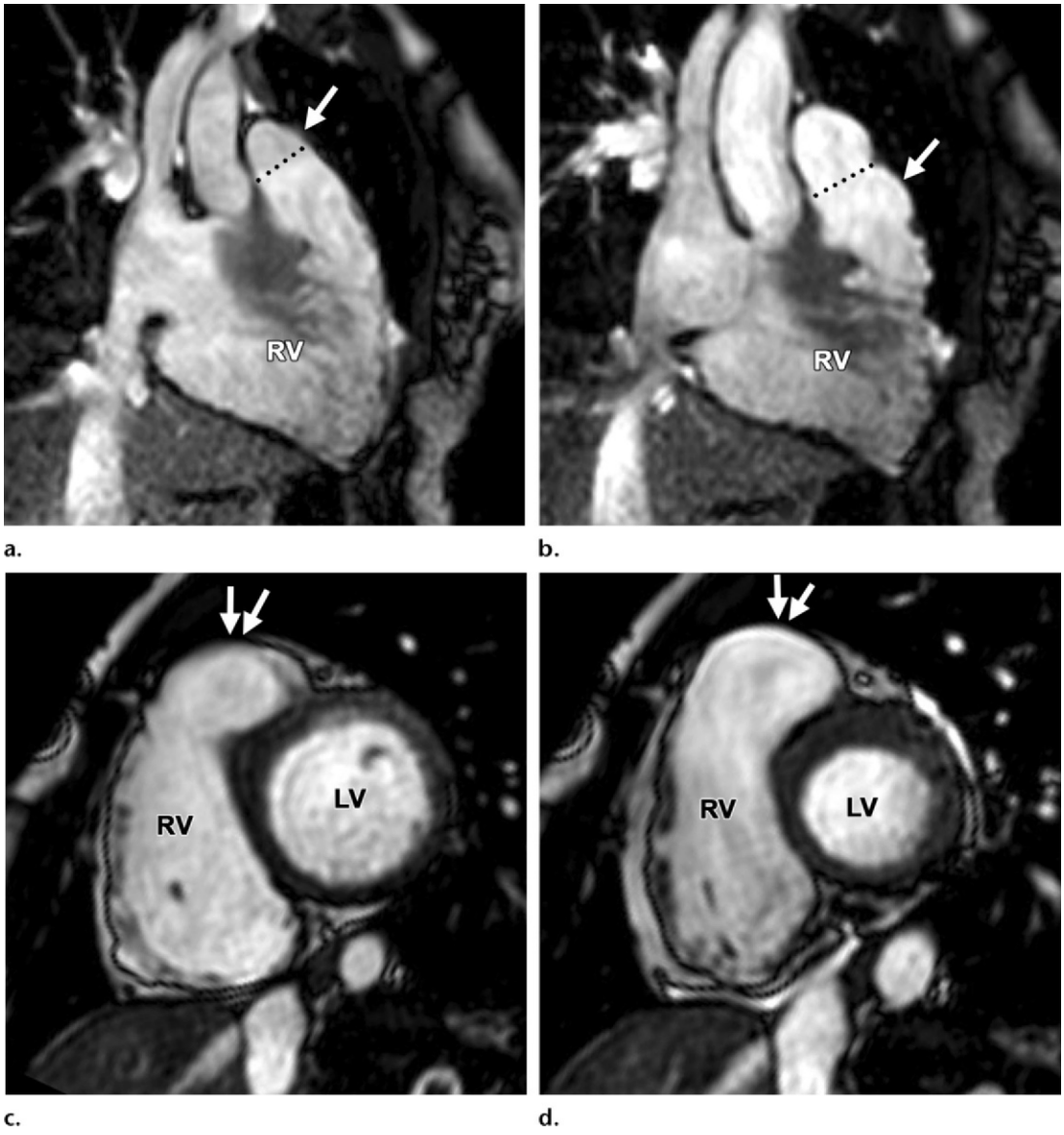


**Figure 11.** RVOT wall motion abnormality in a 36-year-old woman with a history of ARVC. RVOT **(a, b)** and short-axis **(c, d)** bright-blood cine SSFP MR images were obtained in diastole **(a, c)** and in systole **(b, d)**. RVOT dyskinesia (arrows in **c, d**) can be seen at end systole and end diastole. The dotted line **(a, b)** indicates the level of the pulmonary valve annulus. Normal outpouching of the sinuses (arrow in **a**) occurs above the level of the annulus, whereas wall motion abnormalities in ARVC (arrow in **b**) occur below this level. (See Fig 12 for comparison with normal pulmonary valve sinuses.)

(Fig 12) (Movie 6 [online]). Normal motion of the RVOT should be confirmed on the axial images. In our experience, regional dysfunction in the RVOT is rarely an isolated finding in ARVC, and other morphologic and functional abnormalities should be sought to confirm or exclude the diagnosis of ARVC.

## Variants in RV Shape That Simulate RV Dilatation

Dilatation of the RV is an essential component of the diagnosis of ARVC at cardiac MR imaging and is included in the task force criteria. The severity of the RV dilatation will determine if it fulfills major or minor criteria (5). Because RV end-diastolic volume is a function of body size, this parameter is indexed to body surface area. This indexing is applicable to both cardiac MR imaging and echocardiographic measurements. The index was selected on the basis of 108 probands with newly diagnosed ARVC (5). To meet the revised task force criteria with cardiac MR imaging, the combination of *(a)* regional wall motion abnormality and *(b)* either RV dilatation or reduced global RV function is required (Table 1).

Normal variations of RV shape can simulate RV dilatation. Fritz et al (40) evaluated 30 healthy volunteers with cardiac MR imaging and

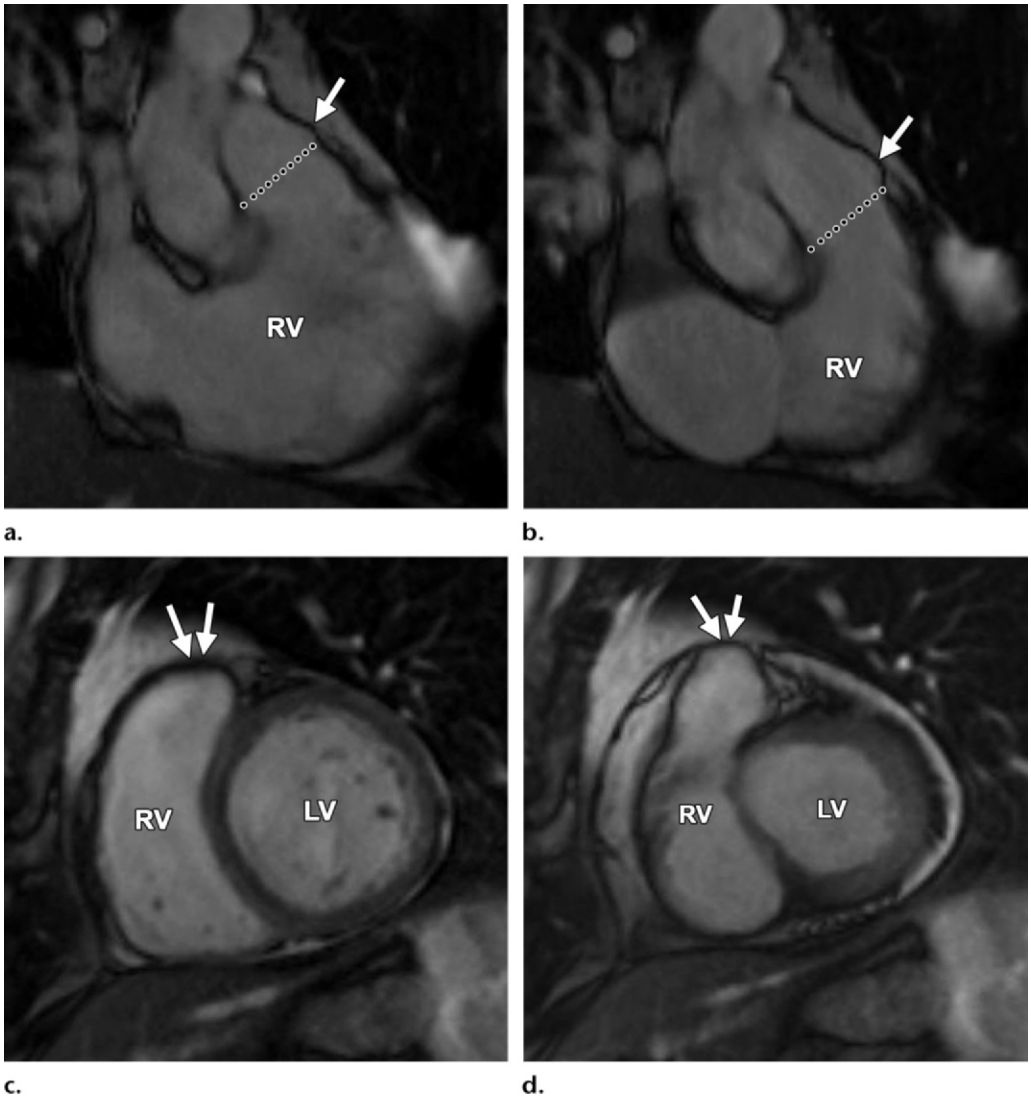


**Figure 12.** Normal pulmonary valve sinuses in a 58-year-old woman. RVOT **(a, b)** and short-axis **(c, d)** bright-blood cine SSFP MR images show normal pulmonary valve sinuses at end diastole **(a, c)** and end systole **(b, d)**. On the short-axis images, the pulmonary valve sinus (arrows in **c, d**) can give the appearance of dyskinetic systolic wall motion. To avoid misdiagnosis, it is important to identify the level of the pulmonary valve annulus (dotted line in **a, b**). Normal outpouching of the sinuses (arrow in **a, b**) occurs above the level of the annulus, whereas wall motion abnormalities in ARVC occur below this level.

described three categories of normal RV shape. These categories include wedge-shaped RV, box-shaped RV, and round RV. A wedge-shaped RV has a straight anterior free wall without any bulging or irregularity. This RV shape is what most imagers would consider the "typical" appearance of a normal RV. A box-shaped RV has bulging of the middle to apical free wall, which creates a squared-off appearance. This variety can be confused with a dilated RV that is due to ARVC. A round RV has a smooth convex curve of the anterior free wall without straight segments or focal outpouching. Figure 13 shows the similarities between the box-shaped RV and the typical appearance of the RV in a patient with ARVC.

## Pathologic Conditions That Mimic Findings in ARVC

### Sarcoidosis

Cardiac sarcoidosis can mimic ARVC in a variety of ways (43). Similar to those with ARVC, patients with cardiac sarcoidosis are at risk for arrhythmias, specifically conduction abnormalities and critical ventricular arrhythmias. Common sites of myocardial involvement are the LV lateral wall and papillary muscles, the basal aspect of the interventricular septum, the RV free wall, and the atrial walls (44). Sarcoidosis can sometimes involve the RV, with considerable overlap in appearance with that of the RV in ARVC. Clinical features and electro-

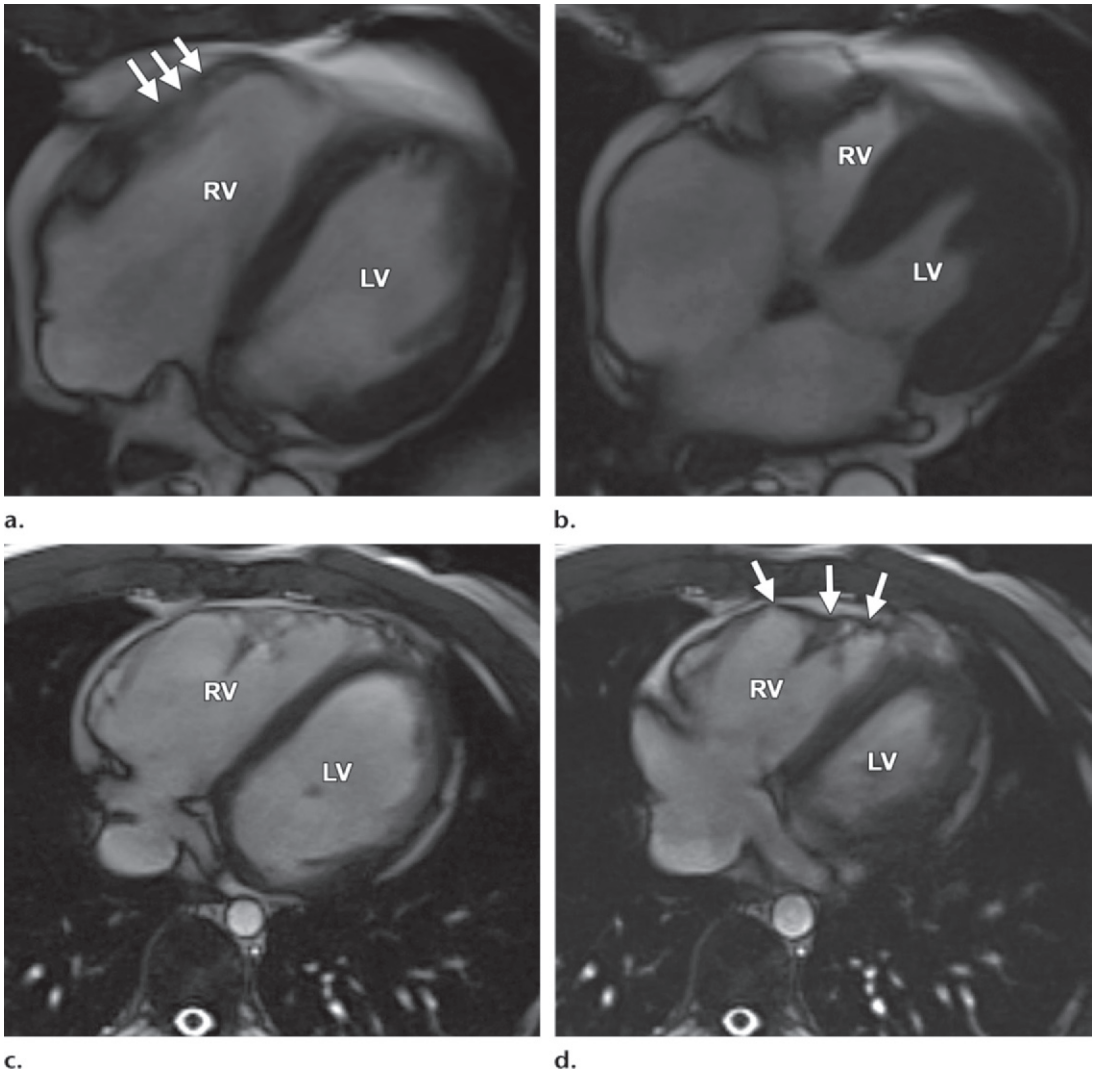


**Figure 13.** Box-shaped RV compared with the typical appearance of the RV in ARVC. **(a, b)** Axial end-diastolic **(a)** and end-systolic **(b)** bright-blood SSFP MR images of a 71-year-old man with no history of ARVC were obtained because of a history of palpitations. **(c, d)** Axial end-diastolic **(c)** and end-systolic **(d)** bright-blood MR images were obtained in a 24-year-old man with ARVC. Note the similarities between the normal-variant box-shaped free wall of the RV (arrows in **a**) and the typical appearance of the bulging RV free wall in ARVC (arrows in **d**).

cardiographic findings are also similar to those in ARVC. Vasaiwala et al (45) showed that 15% of a group of 20 patients who were initially diagnosed with ARVC had sarcoidosis at endomyocardial biopsy. None of these patients had radiographic evidence of sarcoidosis. Two patients with ARVC and one with sarcoidosis had mediastinal lymphadenopathy at cardiac MR imaging. Imaging features of RV sarcoidosis include global hypokinesia, microaneurysms, dilatation, and late myocardial enhancement (Fig 14). Differences in the overall pattern of the distribution of late myocardial enhancement may help distinguish between the two entities. Late myocardial enhancement in cardiac sarcoidosis is patchy and/or linear and subepicardial and/or midmyocardial and typically involves the LV, especially the basal interventricular septum (46). In ARVC, delayed enhancement is typically absent. If it is found in ARVC, late myocardial enhancement may occur in the subtricuspid region, extending anteriorly into the RVOT (23) (Fig 15).

Teaching Point

## Myocarditis

Myocarditis is an inflammatory disorder of the myocardium and is a cause of sudden death in young adults (47). Myocardial inflammation can lead to cell death and replacement fibrosis, resulting in ventricular functional and structural changes (47–49). The range of symptoms extends from no symptoms to severe heart failure or critical arrhythmia (50). In patients with myocarditis, the overlap of the patient demographics, clinical symptoms, electrocardiographic changes, biopsy results, and imaging findings with those of ARVC

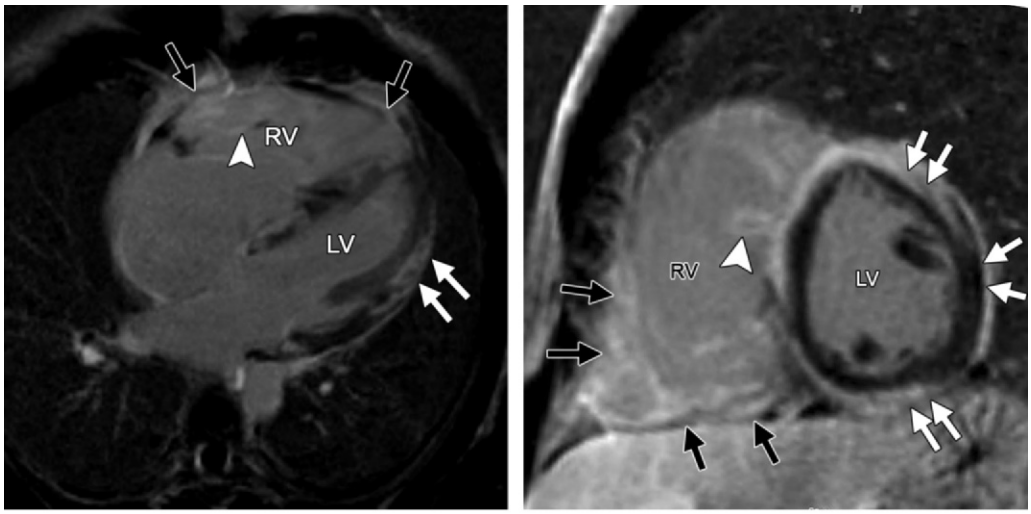


a. b.

**Figure 14.** Delayed enhancement in a 33-year-old man with biopsy-confirmed cardiac sarcoidosis and heart failure. Horizontal long-axis **(a)** and short-axis **(b)** contrast-enhanced phase-sensitive inversion-recovery MR images show patchy delayed enhancement in a nonischemic distribution. The RV is dilated, and there is extensive delayed enhancement of the RV free and inferior walls (black arrows), the subepicardial LV (white arrows), and the trabeculae (arrowhead).

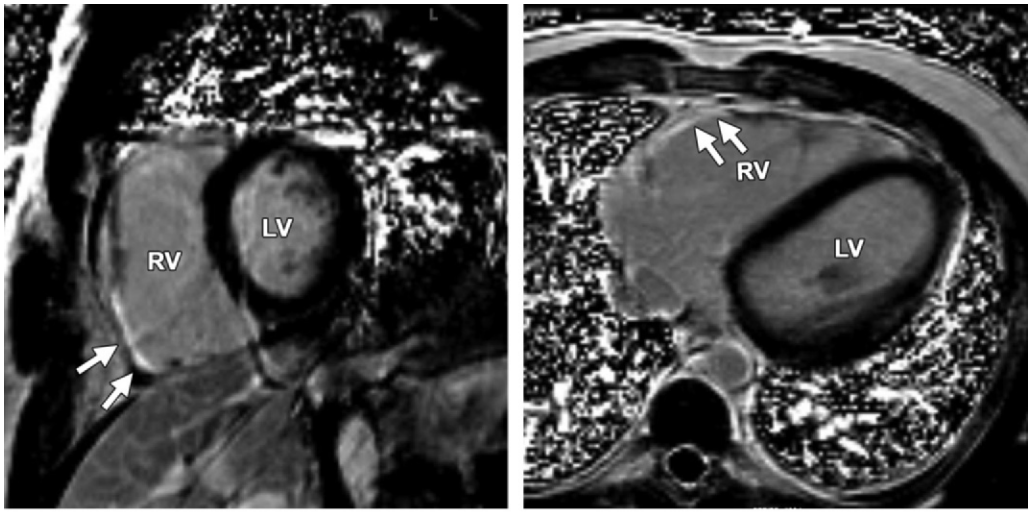


a. b.

**Figure 15.** Delayed enhancement in a 44-year-old man with a history of ARVC. Short-axis **(a)** and axial **(b)** contrast-enhanced inversion-recovery gradient-echo MR images show delayed enhancement in the angle of the RV (arrows in **a**) and in the RV free wall (arrows in **b**).

can lead to a misdiagnosis of ARVC. Late myocardial enhancement is found in the mid wall and/or the subepicardium, most often the lateral and inferior walls of the LV (49) (Fig 16). Myocarditis affecting the RV will result in reduced function and RV dilatation.

In 2009, Pieroni et al (48) compared cardiac MR imaging findings in patients with ARVC with those in patients with myocarditis. Clinical features (with use of the Dallas criteria and the 1994 ARVC task force criteria), the presence and severity of structural and functional RV abnormalities, and the distribution of late myocardial enhancement were similar between the two groups. For example, in the RV, the most common findings in both diseases were regional wall motion abnormalities in the RVOT and anterior free wall. One important distinguishing characteristic of ARVC at cardiac MR imaging was intramyocardial fat deposition, a finding infrequently seen with myocarditis. Unfortunately, as discussed previously, the interpretation of intramyocardial fat depicted on cardiac MR images, especially in the RV, is a common source of diagnostic error. Pieroni et al (48) did note that all patients with myocarditis were asymptomatic and free from arrhythmic events at

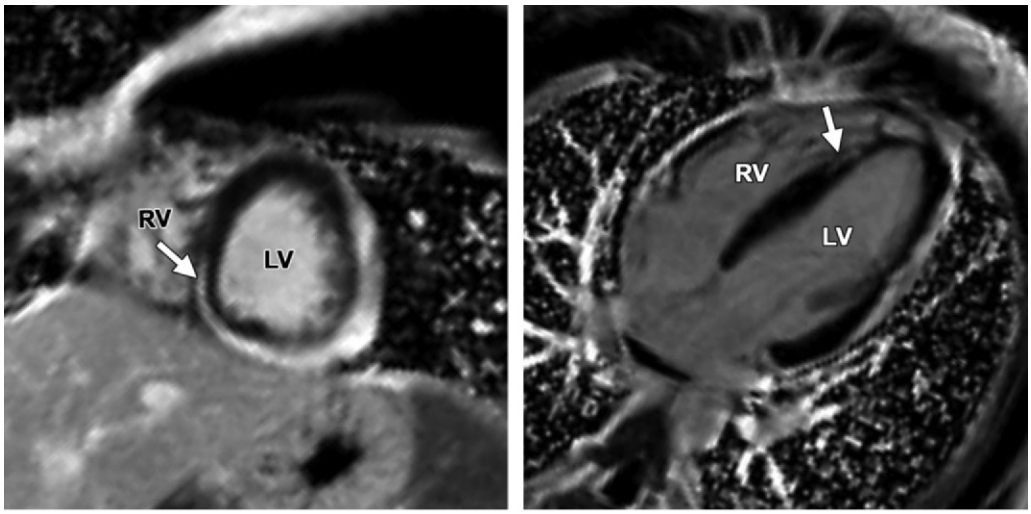


a. b.

**Figure 16.** Delayed enhancement in a 14-year-old male adolescent with acute myocarditis. Short-axis **(a)** and horizontal long-axis **(b)** contrast-enhanced inversion-recovery gradient-echo MR images show extensive circumferential subepicardial delayed enhancement extending to the subendocardial RV side of the interventricular septum (arrow).

follow-up, whereas nearly 50% of patients with ARVC experienced a recurrence of symptomatic ventricular arrhythmias. Therefore, clinical follow-up of patients with ambiguous cardiac MR imaging findings may be helpful in distinguishing between the two entities.

### Pretricuspid Left-to-Right Shunts

Several diseases can cause RV dilatation and critical arrhythmia, but these diseases can be distinguished on the basis of the patient's history and other findings from cardiac MR imaging or other modalities. Partial anomalous pulmonary venous return is one of these diseases that can be misdiagnosed as ARVC.

Shunts commonly result in RV dilatation and, if they are chronic, may result in RV systolic dysfunction. In the vast majority of patients, a left-to-right shunt will be easily diagnosed with echocardiography. However, some types of shunts may be difficult to identify at routine transthoracic echocardiography, such as those associated with partial anomalous pulmonary venous return, an unroofed coronary sinus, or sinus venosus atrial septal defects. The finding of RV dilatation in the absence of an identifiable shunt at echocardiography may lead to referral for a cardiac MR imaging examination to rule out ARVC. Adding to the difficulty is the fact that both groups of patients can present with enlargement of the right atrium and RV and can have atrial and ventricular arrhythmias (51). Standard cardiac MR imaging sequences used in the evaluation for ARVC may not cover the entire thorax and therefore may not allow the depiction of partial anomalous pulmonary venous return (Fig 17). For this reason, we include a set of rapid bright-blood axial MR images through the entire thorax in our ARVC MR imaging protocol to evaluate pulmonary venous connections. In patients with clinical features that overlap between the two diagnoses, it may necessary to perform an echocardiographic bubble study, MR angiography, or computed tomographic angiography to exclude a left-to-right shunt.

## Conclusions

The diagnosis of ARVC with cardiac MR imaging is difficult and, like the diagnosis of other rare conditions, requires imaging experience with the disease. Diagnostic confidence is improved by using objective criteria from the revised task force criteria and using multiple diagnostic criteria, rather than relying on the findings at cardiac MR imaging. When appropriate, second opinions should be sought for difficult cases. Despite the strengths of cardiac MR imaging, the inherent difficulties in the quantitative and qualitative assessment of the RV can lead to a misdiagnosis of ARVC. Several common pitfalls frequently occur in the interpretation of cardiac MR imaging examinations for ARVC. The most common pitfalls, in our experience, are *(a)* erroneous diagnosis of either physiologic or artifactual fat infiltration and *(b)* misinterpretations of normal variants of RV wall motion. Knowledge of the characteristic locations and patterns of fatty infiltration, late myocardial enhancement, myocardial thickness, regional and global wall motion, and morphology in ARVC and its common mimics will help avoid a misdiagnosis. Also, it is necessary to realize that although cardiac MR imaging is a

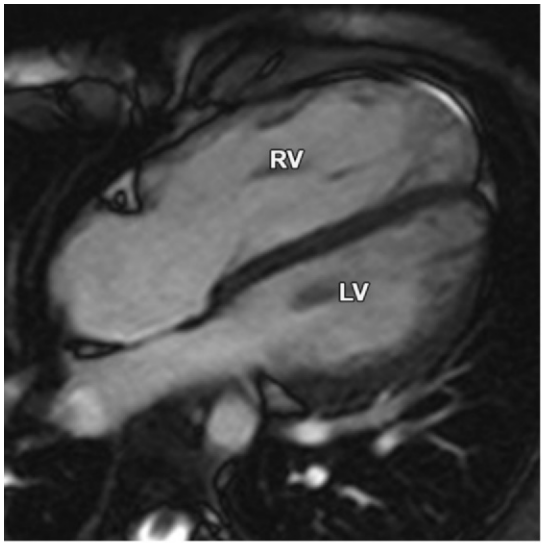


a.

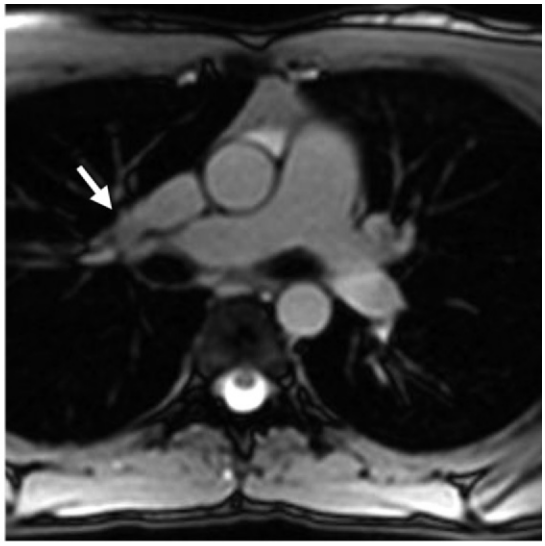

b.

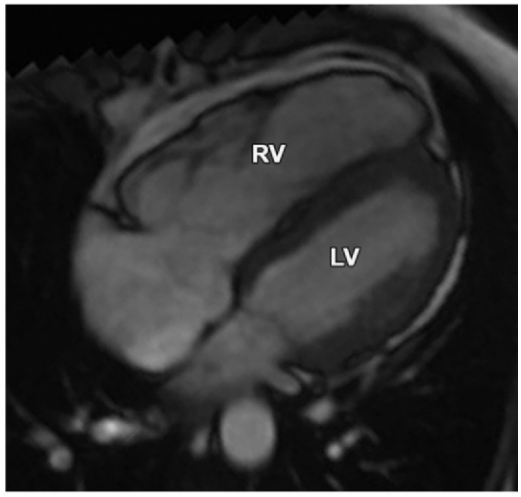


c.

**Figure 17.** Partial anomalous pulmonary venous return compared with ARVC. **(a, b)** Horizontal long-axis bright-blood SSFP **(a)** and axial bright-blood **(b)** MR images of a 16-year-old male adolescent with a history of partial anomalous pulmonary venous return show RV dilatation, with an increase in the transverse chamber diameter. Connection of the pulmonary veins to the superior vena cava (arrow in **b**), instead of the left atrium, is depicted. **(c)** Horizontal long-axis MR image of a 36-year-old woman with a history of ARVC shows that the RV size is similar in patients with ARVC and those with partial anomalous pulmonary venous return.

valuable modality in the diagnosis of ARVC, it is not the reference standard for diagnosis but instead should be used in the context of all available clinical and imaging data. Fat alone should not be considered diagnostic for ARVC, and wall motion abnormalities in the absence of RV dilatation or reduced ejection fraction are not criteria for a diagnosis of ARVC. An understanding of the 2010 task force criteria is critically important for radiologists performing cardiac MR imaging in patients who are suspected of having ARVC.

***Acknowledgments.***—The Johns Hopkins ARVD/C Program is supported in part by the Bogle Foundation, the Healing Hearts Foundation, the Campanella family, the Wilmerding Endowments, and the Dr. Francis P. Chiaramonte Private Foundation.

***Disclosures of Conflicts of Interest.*—H.C.:** *Activities related to the present article:* disclosed no relevant relationships. *Activities not related to the present article:* grants from Medtronic. *Other activities:* disclosed no relevant relationships.

## References

1. Peters S, Trümmel M, Meyners W. Prevalence of right ventricular dysplasia-cardiomyopathy in a non-referral hospital. Int J Cardiol 2004;97(3):499–501.
2. Dalal D, Nasir K, Bomma C, et al. Arrhythmogenic right ventricular dysplasia: a United States experience. Circulation 2005;112(25):3823–3832.
3. Vermes E, Strohm O, Otmani A, Childs H, Duff H, Friedrich MG. Impact of the revision of arrhythmogenic right ventricular cardiomyopathy/dysplasia task force criteria on its prevalence by CMR criteria. JACC Cardiovasc Imaging 2011;4(3):282–287.
4. Bluemke DA. ARVC: imaging diagnosis is still in the eye of the beholder. JACC Cardiovasc Imaging 2011;4(3):288–291.
5. Marcus FI, McKenna WJ, Sherrill D, et al. Diagnosis of arrhythmogenic right ventricular cardiomyopathy/dysplasia: proposed modification of the Task Force Criteria. Eur Heart J 2010;31(7):806–814.
6. Blake LM, Scheinman MM, Higgins CB. MR features of arrhythmogenic right ventricular dysplasia. AJR Am J Roentgenol 1994;162(4):809–812.
7. Sen-Chowdhry S, Morgan RD, Chambers JC, McKenna WJ. Arrhythmogenic cardiomyopathy: etiology, diagnosis, and treatment. Annu Rev Med 2010;61:233–253.
8. Corrado D, Basso C, Thiene G. Sudden cardiac death in young people with apparently normal heart. Cardiovasc Res 2001;50(2):399–408.

9. Hamid MS, Norman M, Quraishi A, et al. Prospective evaluation of relatives for familial arrhythmogenic right ventricular cardiomyopathy/dysplasia reveals a need to broaden diagnostic criteria. J Am Coll Cardiol 2002;40(8):1445–1450.
10. McKenna WJ, Thiene G, Nava A, et al. Diagnosis of arrhythmogenic right ventricular dysplasia/cardiomyopathy. Task Force of the Working Group Myocardial and Pericardial Disease of the European Society of Cardiology and of the Scientific Council on Cardiomyopathies of the International Society and Federation of Cardiology. Br Heart J 1994;71(3):215–218.
11. Cox MG, van der Smagt JJ, Noorman M, et al. Arrhythmogenic right ventricular dysplasia/cardiomyopathy diagnostic task force criteria: impact of new task force criteria. Circ Arrhythm Electrophysiol 2010;3(2):126–133.
12. Tandri H, Macedo R, Calkins H, et al. Role of magnetic resonance imaging in arrhythmogenic right ventricular dysplasia: insights from the North American arrhythmogenic right ventricular dysplasia (ARVD/C) study. Am Heart J 2008;155(1):147–153.
13. Bomma C, Rutberg J, Tandri H, et al. Misdiagnosis of arrhythmogenic right ventricular dysplasia/cardiomyopathy. J Cardiovasc Electrophysiol 2004;15(3):300–306.
14. Bomma C, Dalal D, Tandri H, et al. Regional differences in systolic and diastolic function in arrhythmogenic right ventricular dysplasia/cardiomyopathy using magnetic resonance imaging. Am J Cardiol 2005;95(12):1507–1511.
15. Jain A, Tandri H, Calkins H, Bluemke DA. Role of cardiovascular magnetic resonance imaging in arrhythmogenic right ventricular dysplasia. J Cardiovasc Magn Reson 2008;10:32. http://www.jcmr-online.com/content/10/1/32. Published June 20, 2008. Accessed January 12, 2013.
16. Dalal D, Tandri H, Judge DP, et al. Morphologic variants of familial arrhythmogenic right ventricular dysplasia/cardiomyopathy: a genetics–magnetic resonance imaging correlation study. J Am Coll Cardiol 2009;53(15):1289–1299.
17. Basso C, Thiene G. Adipositas cordis, fatty infiltration of the right ventricle, and arrhythmogenic right ventricular cardiomyopathy: just a matter of fat? Cardiovasc Pathol 2005;14(1):37–41.
18. Burke AP, Farb A, Tashko G, Virmani R. Arrhythmogenic right ventricular cardiomyopathy and fatty replacement of the right ventricular myocardium: are they different diseases? Circulation 1998;97(16):1571–1580.
19. Basso C, Thiene G, Corrado D, Angelini A, Nava A, Valente M. Arrhythmogenic right ventricular cardiomyopathy: dysplasia, dystrophy, or myocarditis? Circulation 1996;94(5):983–991.
20. Thiene G, Nava A, Corrado D, Rossi L, Pennelli N. Right ventricular cardiomyopathy and sudden death in young people. N Engl J Med 1988;318(3):129–133.
21. Kayser HW, van der Wall EE, Sivananthan MU, Plein S, Bloomer TN, de Roos A. Diagnosis of arrhythmogenic right ventricular dysplasia: a review. RadioGraphics 2002;22(3):639–648; discussion 649–650.
22. Kimura F, Matsuo Y, Nakajima T, et al. Myocardial fat at cardiac imaging: how can we differentiate pathologic from physiologic fatty infiltration? RadioGraphics 2010;30(6):1587–1602.
23. Tandri H, Saranathan M, Rodriguez ER, et al. Noninvasive detection of myocardial fibrosis in arrhythmogenic right ventricular cardiomyopathy using delayed-enhancement magnetic resonance imaging. J Am Coll Cardiol 2005;45(1):98–103.
24. Goldfarb JW, Roth M, Han J. Myocardial fat deposition after left ventricular myocardial infarction: assessment by using MR water-fat separation imaging. Radiology 2009;253(1):65–73.
25. Fontaine G, Fontaliran F, Zenati O, et al. Fat in the heart: a feature unique to the human species? observational reflections on an unsolved problem. Acta Cardiol 1999;54(4):189–194.
26. Raney AR, Saremi F, Kenchaiah S, et al. Multidetector computed tomography shows intramyocardial fat deposition. J Cardiovasc Comput Tomogr 2008;2(3):152–163.
27. Jacobi AH, Gohari A, Zalta B, Stein MW, Haramati LB. Ventricular myocardial fat: CT findings and clinical correlates. J Thorac Imaging 2007;22(2):130–135.
28. Baroldi G, Silver MD, De Maria R, Parodi O, Pellegrini A. Lipomatous metaplasia in left ventricular scar. Can J Cardiol 1997;13(1):65–71.
29. Marcus F, Basso C, Gear K, Sorrell VL. Pitfalls in the diagnosis of arrhythmogenic right ventricular cardiomyopathy/dysplasia. Am J Cardiol 2010;105(7):1036–1039.
30. Castillo E, Tandri H, Rodriguez ER, et al. Arrhythmogenic right ventricular dysplasia: ex vivo and in vivo fat detection with black-blood MR imaging. Radiology 2004;232(1):38–48.
31. Araoz PA, Mulvagh SL, Tazelaar HD, Julsrud PR, Breen JF. CT and MR imaging of benign primary cardiac neoplasms with echocardiographic correlation. RadioGraphics 2000;20(5):1303–1319.
32. Sparrow PJ, Kurian JB, Jones TR, Sivananthan MU. MR imaging of cardiac tumors. RadioGraphics 2005;25(5):1255–1276.
33. Heyer CM, Kagel T, Lemburg SP, Bauer TT, Nicolas V. Lipomatous hypertrophy of the interatrial septum: a prospective study of incidence, imaging findings, and clinical symptoms. Chest 2003;124(6):2068–2073.
34. Adriaensen ME, Schaefer-Prokop CM, Duyndam DA, Zonnenberg BA, Prokop M. Fatty foci in the myocardium in patients with tuberous sclerosis complex: common finding at CT. Radiology 2009;253(2):359–363.
35. Macedo R, Prakasa K, Tichnell C, et al. Marked lipomatous infiltration of the right ventricle: MRI findings in relation to arrhythmogenic right ventricular dysplasia. AJR Am J Roentgenol 2007;188(5):W423–W427.
36. Bluemke DA, Krupinski EA, Ovitt T, et al. MR imaging of arrhythmogenic right ventricular cardiomyopathy: morphologic findings and interobserver reliability. Cardiology 2003;99(3):153–162.
37. Tansey DK, Aly Z, Sheppard MN. Fat in the right ventricle of the normal heart. Histopathology 2005;46(1):98–104.
38. Brochhausen C, Turial S, Müller FK, et al. Pectus excavatum: history, hypotheses and treatment options. Interact Cardiovasc Thorac Surg 2012;14(6):801–806.
39. Sievers B, Addo M, Franken U, Trappe HJ. Right ventricular wall motion abnormalities found in healthy subjects by cardiovascular magnetic reso-

nance imaging and characterized with a new segmental model. J Cardiovasc Magn Reson 2004;6(3):601–608.
40. Fritz J, Solaiyappan M, Tandri H, et al. Right ventricle shape and contraction patterns and relation to magnetic resonance imaging findings. J Comput Assist Tomogr 2005;29(6):725–733.
41. Tandri H, Castillo E, Ferrari VA, et al. Magnetic resonance imaging of arrhythmogenic right ventricular dysplasia: sensitivity, specificity, and observer variability of fat detection versus functional analysis of the right ventricle. J Am Coll Cardiol 2006;48(11):2277–2284.
42. Santos A, Thomas B, Tavares NJ. The right ventricular outflow tract in patients with suspected arrhythmogenic right ventricular cardiomyopathy referred for cardiac magnetic resonance imaging. Rev Port Cardiol 2008;27(3):335–338.
43. Yared K, Johri AM, Soni AV, et al. Cardiac sarcoidosis imitating arrhythmogenic right ventricular dysplasia. Circulation 2008;118(7):e113–e115. http://circ.ahajournals.org/content/118/7/e113.long. Accessed January 12, 2013.
44. Silverman KJ, Hutchins GM, Bulkley BH. Cardiac sarcoid: a clinicopathologic study of 84 unselected patients with systemic sarcoidosis. Circulation 1978;58(6):1204–1211.
45. Vasaiwala SC, Finn C, Delpriore J, et al. Prospective study of cardiac sarcoid mimicking arrhythmogenic right ventricular dysplasia. J Cardiovasc Electrophysiol 2009;20(5):473–476.
46. Vignaux O. Cardiac sarcoidosis: spectrum of MRI features. AJR Am J Roentgenol 2005;184(1):249–254.
47. Feldman AM, McNamara D. Myocarditis. N Engl J Med 2000;343(19):1388–1398.
48. Pieroni M, Dello Russo A, Marzo F, et al. High prevalence of myocarditis mimicking arrhythmogenic right ventricular cardiomyopathy: differential diagnosis by electroanatomic mapping-guided endomyocardial biopsy. J Am Coll Cardiol 2009;53(8):681–689.
49. Kindermann I, Barth C, Mahfoud F, et al. Update on myocarditis. J Am Coll Cardiol 2012;59(9):779–792.
50. Dec GW Jr, Palacios IF, Fallon JT, et al. Active myocarditis in the spectrum of acute dilated cardiomyopathies: clinical features, histologic correlates, and clinical outcome. N Engl J Med 1985; 312(14):885–890.
51. Chu AF, Zado E, Marchlinski FE. Atrial arrhythmias in patients with arrhythmogenic right ventricular cardiomyopathy/dysplasia and ventricular tachycardia. Am J Cardiol 2010;106(5):720–722.

# Cardiac MR Findings and Potential Diagnostic Pitfalls in Patients Evaluated for Arrhythmogenic Right Ventricular Cardiomyopathy

*Neda Rastegar, MD • Jeremy R. Burt, MD • Celia P. Corona-Villalobos, MD • Anneline S. te Riele, MD • Cynthia A. James, PhD • Brittney Murray, MS • Hugh Calkins, MD • Harikrishna Tandri, MD • David A. Bluemke, MD, PhD • Stefan L. Zimmerman, MD • Ihab R. Kamel, MD, PhD*

**RadioGraphics 2014;** 34:1553–1570 • **Published online** 10.1148/rg.346140194 • **Content Codes:** CA MR

**Page 1558**
We recommend the evaluation of fibrofatty infiltration only as a secondary assessment after the evaluation of the more reliable functional and structural assessment of the RV as defined by the task force criteria.

**Page 1559**
Physiologic fat usually spares the subendocardium and characteristically increases the total thickness of the involved myocardium.This is in contrast to ARVC, in which fat replaces normal myocardium, resulting in an unchanged or thinner wall thickness.

**Page 1559**
At cine imaging, the tethered portion of the RV free wall remains static in location, whereas the adjacent RV myocardium contracts normally.

**Page 1560**
Pectus excavatum deformity of the chest wall, which is reported to account for 90% of cases of congenital chest wall deformity, results in restricted motion of the basolateral and inferolateral walls of the RV. Pectus excavatum also causes narrowing of the RV base and relative enlargement of the RV apex and the RVOT, potentially leading to a misdiagnosis of ARVC.

**Page 1565**
Late myocardial enhancement in cardiac sarcoidosis is patchy and/or linear and subepicardial and/or midmyocardial and typically involves the LV, especially the basal interventricular septum.